Detailed analysis of the influence of an inductively coupled plasma reactive-ion etching process on the hole depth and shape of photonic crystals in InP/InGaAsP

P. Strasser,[a] R. Wüest, and F. Robin
Communication Photonics Group, Electronics Laboratory (IfE), ETH Zurich, CH-8092 Zurich, Switzerland

D. Erni
General and Theoretical Electrical Engineering (ATE), Faculty of Engineering, University of Duisburg-Essen, D-47048 Duisburg, Germany

H. Jäckel
Communication Photonics Group, Electronics Laboratory (IfE), ETH Zurich, CH-8092 Zurich, Switzerland

(Received 5 October 2006; accepted 30 January 2007; published 6 March 2007)

The authors report on the fabrication of photonic crystals in the InP/InGaAsP/InP material system for applications at telecommunication wavelengths. To achieve low optical loss, the photonic crystal holes must demonstrate smooth sidewalls and should be simultaneously deep and cylindrical. The authors present the etching process of these structures based on a $Cl_2/Ar/N_2$ chemistry with an inductively coupled plasma reactive-ion etching system. A systematic analysis is provided on the dependency of the hole sidewall roughness, depth, and shape on the process parameters such as etching power, pressure, and chemical composition of the plasma. They found that a low plasma excitation power and a low physical etching are beneficial for achieving deep holes, whereas for the nitrogen content in the plasma, a delicate balance needs to be found. Nitrogen has a negative impact on the hole shape and surface roughness but is capable of preventing underetching below the mask by passivation of the sidewalls. With the authors' process more than 4 μm deep holes with low conicity have been demonstrated. © *2007 American Vacuum Society.* [DOI: 10.1116/1.2712198]

I. INTRODUCTION

Photonic crystal (PhC) devices have gained a large interest as they offer the possibility to tailor the dispersion relation of light and to achieve ultracompact devices and new optical features.[1–3] Planar PhC (PPhCs) are often studied as they are relatively easy to fabricate using standard semiconductor technology. In PPhCs, light is controlled by the PhC in the horizontal direction, whereas the guiding in the vertical direction relies on total internal reflection, either within a membrane (air/semiconductor/air) or a semiconductor layer stack. InP (Refs. 4–6) or GaAs are suitable materials for the fabrication of PPhCs due to the possibility to monolithically integrate optically active and passive sections on the same chip. We fabricate PPhCs in the InP/InGaAsP/InP low refractive index system for the telecommunication wavelengths ($\lambda = 1550$ nm). The main challenge of this vertical layer stack is the low refractive index contrast ($n_{InP} = 3.17$, $n_{InGaAsP} = 3.35$, $\Delta n = 0.18$). Therefore, the vertical light mode extends several micrometers deep into the substrate[7] and holes with diameters of 200–500 nm have to be etched deeper than ~2.5 μm (Refs. 6 and 8) for passive devices to ensure a sufficient overlap of the holes with the optical field. For electrically pumped active devices a thick upper cladding is commonly used to reduce absorption by the metallic contacts, and therefore PhC holes deeper than 4 μm are required typically.

An important criterion for PhC-based waveguides is a low propagation loss,[9–11] e.g., for light traveling along W1 (Ref. 12) waveguides (PhC waveguides with one missing row of holes). Propagation losses originate from sidewall roughness, and vertically tapered or shallow holes.[10] Therefore, the PhC holes need to be simultaneously cylindrical, very deep, and with a smooth surface. Because low-damage dry-etch processes that yield smooth surfaces are not suitable for deep etching, it is not possible to optimize all three criteria simultaneously. Depending on the application, however, their relative weighting is different. For membrane-type PhCs hole depth is not an issue, but the sidewalls need to be very vertical and with low roughness. For active applications hole depth is crucial. Smooth sidewalls are also important to avoid a reduction of the carrier lifetime at surface defects.[13] Overall, the knowledge of the dependence of these hole characteristics on the process parameters is crucial for an application-specific process optimization.

In this article, we report on the influence of process parameters for the inductively coupled plasma (ICP) reactive-ion etching (RIE) of PhC holes in InP/InGaAsP/InP layers on InP substrates. The samples were etched with various process parameters and the hole shape, depth, and surface roughness were evaluated by scanning electron microscopy. To the best of our knowledge, this is the first detailed investigation on the impact of the ICP process parameters based on a $Cl_2/Ar/N_2$ chemistry on the PhC hole quality. In this article, we will first discuss the fabrication and the characterization of the samples. We will then present our findings

[a]Electronic mail: strasser@ife.ee.ethz.ch

TABLE I. Ranges of process parameters for the DOE runs and the derived parameters for the subsequent investigations, including the improvements from Ref. 14.

	Process parameters		
Parameter	DOE	Optimized process	Unit
Cl_2 flux	10	10 or 15	SCCM
Total neutral flux	7–16	~7.1	SCCM
% of N_2 in the neutrals	0%–100%	~30%	
Ar flux	7–16	5	SCCM
N_2 flux	7–16	~2.1	SCCM
He flux	0	15	SCCM
ICP power	1000–2000	600	W
rf power	140–215	160	W
Pressure	3–6	2.2	mTorr
Stage temperature	200	200	°C

regarding the etching of large-area structures, followed by description of the effect of the etching parameters on the resulting holes. Finally, we present the high quality holes we achieved with the optimized process.

II. SAMPLE FABRICATION AND EXPERIMENT

Details of the sample fabrication have been published elsewhere.[14] The wafer growth, mask fabrication, electron beam lithography (EBL) exposure, and mask etching were kept identical for all experiments. Samples were fabricated both in pure InP and in an InP (200 nm)/InGaAsP (400 nm, $n=3.35$)/InP vertical layer stack grown by metal-organic vapor phase epitaxy.[15] Both InP and InP/InGaAsP/InP samples were covered with silicon nitride (SiN_x), a thin titanium film, and an electron beam resist (polymethylmetacrylate). After EBL exposure of 100 $\times 30$ μm^2 arrays of holes of different lattice constants with a filling factor (percentage covered by holes of a unit cell) of 35%, the pattern was transferred by RIE into the silicon nitride.[16] The 400 nm thick SiN_x layer acts as the hard etching mask for the subsequent semiconductor etching in the ICP-RIE.

The ICP-RIE was performed on a Plasmalab 100 system from Oxford Instruments. The samples were glued on top of a 500 μm thick 4 in. silicon carrier wafer with Dow Corning vacuum grease. The etching time was kept constant within the series of samples. The grease was removed after etching using trichloroethylene, and the samples were cleaved through the PhC structures. The structures were imaged with a scanning electron microscope (SEM) Zeiss Ultra 55 with Gemini electron optics and 1.5 nm resolution.

The process optimizations are based on the *design of experiment* (DOE) approach.[14,17] With the DOE technique, a subset of parameter combinations is chosen instead of processing all possible combinations. The distribution of this subset in the parameter landscape is chosen to be evenly distributed. The influence of a process parameter is calculated by averaging the results of the individual samples with the same value for this process parameter. The even distribution of the parameter combinations in the parameter space guarantees to a certain extent the elimination of the influence of the other process parameters during averaging. The DOE technique allows one to gain a comprehensive overview over the relative influence of the process parameters on the hole properties with only a few experiments. For a fine-tuning of the etching recipe, a systematic scan of the region of interest in the parameter landscape is mandatory, as the interaction between the process parameters is very complex.

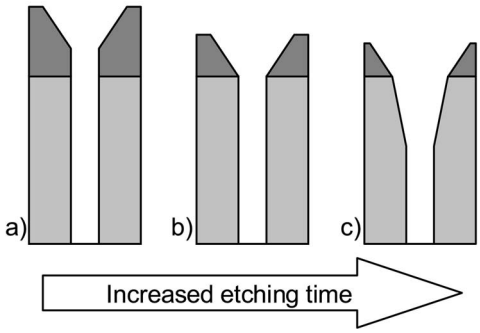

FIG. 1. Schematics of mask erosion. The mask edge is etched faster than the top, resulting in the tapering of the mask (a). As soon as the faceting reaches the semiconductor, the etching has to be stopped (b) to prevent transferring of the faceting into the InP layers and tapering of the holes (c).

For etching of InP, different plasma chemistries have been studied. Well known are CH_4-containing[18] and pure Cl_2-based[19,20] chemistries. However, even low methane fluxes strongly lower the etch rate of InGaAsP layers, and therefore etching deep holes in the InP/InGaAsP/InP structure is not possible.[14] We therefore concentrate our analysis on the Cl_2-based chemistry in this article.

The DOE runs use the parameters shown in Table I. While keeping the Cl_2 flux constant, pressure, ICP and rf powers, and amount and composition of the neutrals were varied. An L16 (Ref. 17) DOE was used, allowing us to evaluate the five input parameters over four equidistant setting values with only 16 etching runs.

As we will show later, sidewall passivation is crucial for PhC etching with Cl_2. The etching product $InCl_x$ could be used for sidewall passivation, as its sublimation temperature in the low-pressure reactor is around 150 °C.[21] However, balancing the amount of passivation with temperature is difficult to achieve as an accurate temperature control of the sample is not possible. Therefore the temperature was chosen to be 200 °C, above the temperature for the $InCl_x$ sublimation, and sidewall passivation was provided by nitrogen addition.

III. EVALUATION METHOD

All quantities of interest are measured using SEM micrographs which have the advantage of a fast *in situ* characterization technique compared to time-consuming optical characterization by, e.g., the internal light source[15] or the end

TABLE II. Influence of the process parameters on quantities of interest for large-area etching. ↗ and ↘ indicate a larger parameter value to be beneficial and detrimental, respectively. The number of arrows relates to the strength of the trend. For the sidewall angle verticality is optimal. Therefore ↗/↘ means that higher parameter values lead to a smaller/larger angle between the sidewall and the plumb line.

	ICP power	rf power	Neutral flux	% of N_2
Sidewall angle			↘↘	↘↘↘
Surface quality				↘↘
Sidewall quality	↗	↗	↘	↘
Maximal achievable etch depth/selectivity against the mask			↘	↘

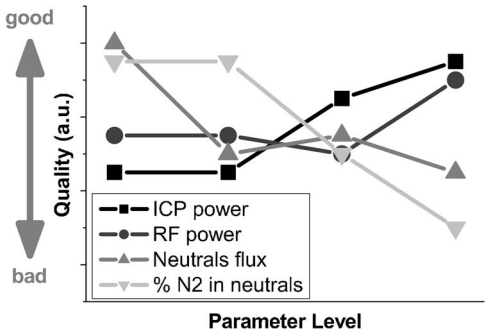

FIG. 3. Influence of the process parameter on the sidewall quality. The parameter levels are according to Table I: ICP power of 1000–2000 W, rf power of 140–215 W, neutral flux of 7–15 SCCM, and N_2 percentage of 0%–100%.

fire[7] techniques, although they do not deliver loss figures for PhC waveguides. They, however, provide an accurate three-dimensional picture of the exact hole geometry. The link between the extracted figures of merit from SEM images and the loss values has to be made using a corresponding set of optical calibration experiments or with theoretical loss models,[10,11] where loss caused by hole depth and conical shape can be predicted.

Next to the standard quantities of interest in process development such as *InP* and *InGaAsP etch rates, sidewall angles*, and *mask etch rate*, some additional figures of merit for this investigation have been defined as follows:

1. *Mask selectivity*=(InP etch rate)/(mask etch rate).
2. *Quaternary material selectivity*=(InGaAsP etch rate)/(InP etch rate).
3. The *extrapolated maximal etch depth (eMED)* =(measured depth)[total mask thickness/(total mask thickness)−(remaining mask thickness)] accounts for a longer etching time due to the remaining mask material after the etching. This figure of merit is computed as all samples were etched for 90 s, and depending on the recipe, the plasma may be diversely aggressive against the mask. The eMED is calculated based on the measured large area or hole depth and the remaining mask thickness at the structure edge, as mask faceting (Fig. 1) is the limiting factor for the etching time. The eMED calculation has, however, a limited accuracy of ±400 nm as the measurement of the remaining mask thickness is unreliable due to the mask rounding off at the facet. Additionally, for holes the etching rate may slow down with increasing depth due to aspect-ratio dependent etch rates.[22]
4. *Surface roughness, hole shape*, and *undercut*[8] are quantified by comparing and ranking the SEM micrographs.

IV. LARGE-AREA ETCHING PROPERTIES OF A $Cl_2/Ar/N_2$ PLASMA

During the PhC device fabrication for optical port-to-port end fire measurements,[7] photonic wires (PhWs) are etched simultaneously with the PhC holes. Of special interest for PhWs is the etch depth, the roughness of the etched bottom surface and of the sidewalls, and the verticality of the sidewalls.

The impact of the etching parameters is summarized in Table II. Both high rf and ICP powers are beneficial for sidewall quality, whereas a high neutral flux and a high nitrogen content have a negative overall impact on all figures of interest.

Before further analysis, we should mention that increasing the percentage of N_2 in the neutrals has two effects: (i) it

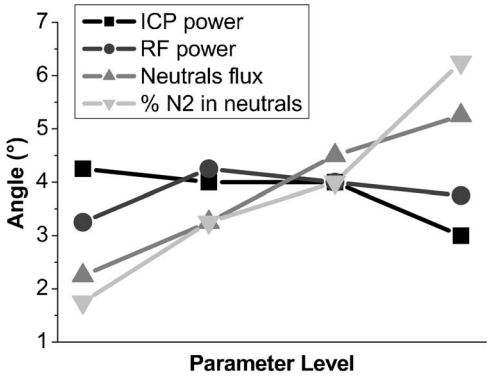

FIG. 2. Influence of the process parameters on the sidewall angle. The parameter levels are according to Table I: ICP power of 1000–2000 W, rf power of 140–215 W, neutral flux of 7–15 SCCM, and N_2 percentage of 0%–100%.

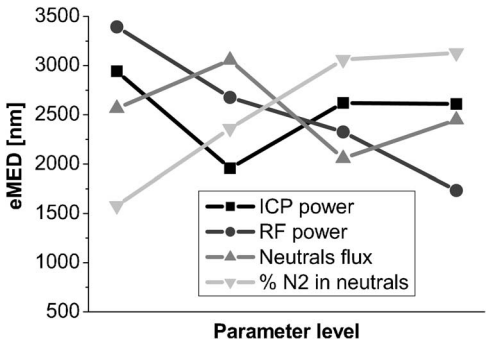

FIG. 4. Influence of the process parameter on the eMED for ⌀200 nm holes. The parameter levels are according to Table I: ICP power of 1000–2000 W, rf power of 140–215 W, neutral flux of 7–15 SCCM, and N_2 percentage of 0%–100%.

TABLE III. Influence of the process parameters on quantities of interest for PhC hole etching. ↗ and ↘ indicate a larger parameter value to be beneficial and detrimental, respectively. For holes, the absence of undercut is optimal. Therefore ↗ and ↘ mean that higher parameter values enhance and reduce the undercut, respectively. The number of arrows relates to the strength of the trend.

	ICP power	rf power	Neutral flux	% of N_2	Pressure
eMED	↘	↘↘	↘	↗↗	
Hole shape conicality	↗		↘	↘	
Undercut				↘↘	↗
Hole surface quality		↗		↘	
Grasslike vertical stripes on the surface				↘	

passivates the sidewalls and the surface by preferentially forming N–P bonds and therefore inhibits Cl_2–In bonds[19,23] and (ii) it reduces the sputter efficiency of the total neutral flux, as heavy argon ions (atomic mass: 40) are replaced by light nitrogen (atomic mass: 14) ions.

All measured values for the etch rates in this DOE run lie between 1 and 3 μm/min. While higher rf and ICP powers increase the etch rate, they do not improve the maximum achievable etch depth, as the mask is also etched faster. On the other hand, a high chemical content in the plasma is advantageous for a larger etch depth due to the enhanced selectivity of the chemical etching processes against the mask. In addition, the sidewall passivation by nitrogen,[19] which enhances micromasking and results in a rough bottom surface and reduced maximal etch depth, is limited. It should be mentioned that reducing the neutral flux is equivalent to increasing the Cl_2 flux, as the total flux has a negligible impact on the etching result.

Figure 2 presents the influence of the process parameters on the sidewall angle based on the DOE evaluation. The neutral content and the amount of N_2 in the plasma predominantly determine the sidewall angle. Indeed, by adding neutrals or passivating sidewalls with nitrogen, we reduce the chemical etching by chlorine ions and therefore less vertical sidewalls are obtained. Underetching is not observed.

The chemical composition of the plasma has the most pronounced influence on the quality of the etching, as shown in Table II. Whereas the bottom etched surface quality is mainly determined by the nitrogen content in the plasma due to passivation of the surface and the subsequent micromasking or grass formation, the sidewall quality is in addition positively influenced by a high ICP power and a low neutral flux (Fig. 3).

We found no distinct influence of the process parameter on the quaternary material selectivity. The value for the quaternary material selectivity lies mostly between 0.8 and 0.9 over the 16 etching experiments of the L16 DOE in contrast to methane-based plasmas for which the selectivity is 0.25.[18] Also pressure has no significant influence on any quantity of interest.

V. HOLE ETCHING

For holes, the figures of merit are hole shape, surface roughness, and hole depth. Typical hole diameters for wavelengths of $\lambda = 1550$ nm are in the range of 150–500 nm. In addition, a low quaternary material selectivity is favorable to avoid differential etching of the core and the claddings.

The qualitative behavior of the etching is assumed to be independent of the hole size and thus the measured values can be averaged over different diameters. Table III summarizes the impact of the process parameters on the hole characteristics. Again, the pressure has a minor impact except for undercut.

A. Hole depth

Figure 4 shows the impact of the process parameters on the eMED for ⌀200 nm holes. The trends are similar for ⌀500 nm holes.

The calculated eMED ranges in the individual runs of the DOE are 0.8–4.4 μm and 1.3–4.8 μm for ⌀200 and hole ⌀500 nm holes, respectively.

Whereas nitrogen has a negative impact on the eMED for large-area etching (Table II) due to micromasking, it is beneficial for holes (Table III and Fig. 4). These seemingly contradictory results can be explained as follows: due to the enhanced surface passivation with higher nitrogen content,

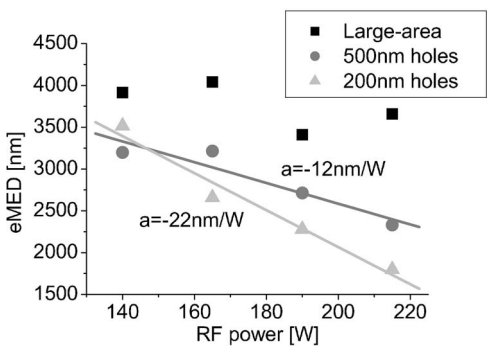

FIG. 5. Correlation between the rf power and eMED for large-area structures and two different hole sizes.

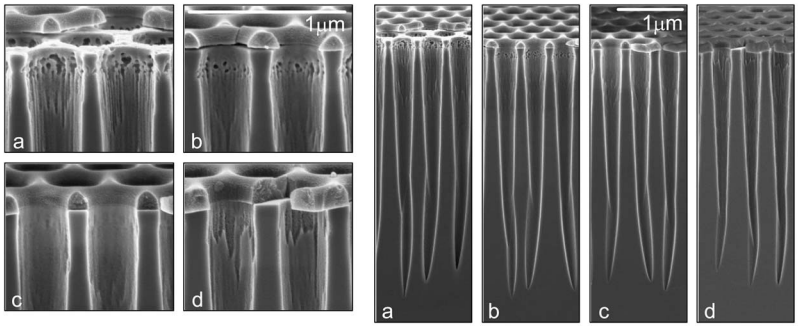

FIG. 6. Holes etched with a $Cl_2/Ar/N_2/He$ process (Ref. 14). The nitrogen flow is varied from 1.3, 2.1, and 2.9 SCCM to 6 SCCM for (a) to (d), respectively. All other process parameters are kept constant. The Cl_2 and Ar fluxes are 15 and 5 SCCM, respectively. All related images have the same scale.

ions are deflected toward the center of the holes. The augmented ion bombardment allows cracking of the passivation layer at the bottom and increases the overall etching rate. The drawback is a more conical shape as will be shown in the next section.

Comparing Table II with Table III and Fig. 4, the rf and ICP powers have a more significant influence on the hole depth than for large-area etching, for which no clear effect was observed. A low power is favorable for deep hole etching, unambiguously for the rf power, and less pronounced in the case of ICP power. This behavior cannot be explained by a selectivity enhancement against the mask due to a lower dc bias as we do not observe a reduction in etch depth for higher power in the case of large-area etching. We explain this phenomenon as follows:

At higher power, the plasma density and the amount of active species accelerated towards the sample are increased. This enhances the etch rate of the semiconductor but also the etch rate of the mask. Whereas this is not a limitation in etching large-area openings, it gets increasingly difficult to diffuse neutral etch species into or remove the etch products out of the high-aspect-ratio holes, and therefore the etching rate slows down when the holes get deeper. This hypothesis is supported by the fact that the hole depth reduction at higher power is more pronounced for small holes as shown in Fig. 5. For large-area structures, a slight decrease with the power of the eMED is observed, which can be caused by other parameters in the DOE. For holes, we measure a clear decrease of the eMED with increasing rf powers of 12 and 22 nm/W for ⌀500 and ⌀200 nm holes, respectively.

The ICP power shows less influence on the hole depth. While a lower rf power not only reduces the plasma density but also the dc bias, a lower ICP power reduces the plasma density but increases the dc bias, leading to a higher sputter efficiency of the mask. This reduces the selectivity of InP against the mask and the eMED.

B. Hole quality

All quantities of interest (hole shape, sidewall roughness, undercut) are strongly influenced by the nitrogen content in the neutral flux. The impact of nitrogen on the sidewall passivation of the holes and of large-area structures and the reduction of the undercut will now be discussed. As will be shown later, a higher Cl_2 flux increases the undercut while this effect is not seen for a lower neutral content. The effect

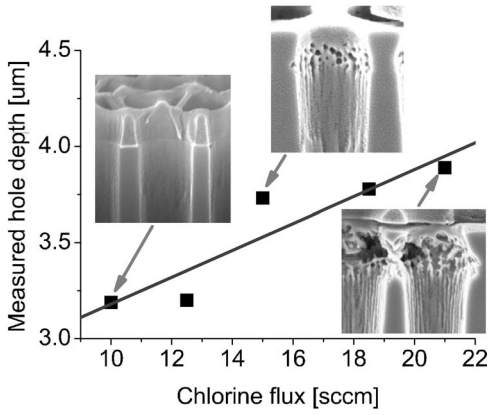

FIG. 7. Depth of holes etched with a $Cl_2/Ar/N_2/He$ process (Ref. 14) vs Cl_2 flux. All other parameters are kept constant. The N_2 and Ar fluxes are 2.1 and 5 SCCM, respectively. The pressure is 2.2 mTorr except for the highest flux where it is increased to 2.5 mTorr. Insets: SEM micrographs of the hole cross sections and the undercut.

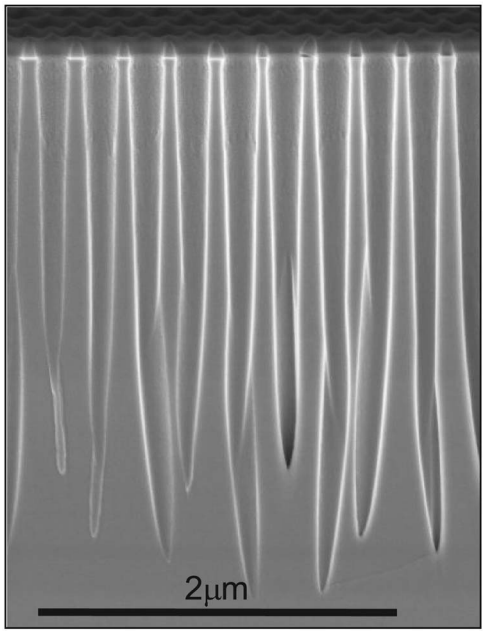

FIG. 8. PhC etched in InP. The holes have a diameter of 180 nm and a depth of 2.9 μm, resulting in an aspect ratio of 1:16.

TABLE IV. Dependencies and the effects of the process parameters on PhC holes.

Parameter	Function	Result
Power	Determines plasma density	Reduces eMED due to exhaust limitations
		Enhances the surface quality
Pressure		Prevents undercut at low pressure
Argon	Physical etching	Sputters the mask, dilutes the plasma
Nitrogen	Sidewall passivation	Prevents undercut
	Lower chemical etching	Decreases the quality of the holes due micromasking and passivation
Chlorine	Physical and chemical etching	Produces deep holes, favors undercut

is shadowed in the DOE run by the strong impact of N_2 and the strong correlation between the neutral flux and the content of N_2 in the neutrals.

VI. SIDEWALL PASSIVATION

Besides the DOE runs, additional investigations showed that N_2 prevents undercuts just below the SiN_x mask [Figs. 6(a) and 6(b)]. As the undercut is only visible in holes but not at the sidewalls of large-area structures, we believe that it is caused by the deflection of the incoming chlorine ions from the opposite sidewalls.[8] As the mode intensity at the top of the holes is relatively strong due to the asymmetric slab waveguide structure,[7] the undercut may significantly contribute to optical scattering losses due to its very rough surface. The nitrogen passivation can prevent undercuts as shown in Fig. 6 by formation of N–P bonds at the sidewalls.[19,23] On the other hand too large nitrogen fluxes increase the sidewall roughness and the hole conicity [Fig. 6(d)].

As shown in Fig. 7, with an increased amount of chlorine (which has the same effect as decreasing the overall neutral flux), the etch depth is improved, but more nitrogen is necessary to prevent the undercut at the top of the holes. Also, the small N_2 flux of 2.1 SCCM (SCCM denotes cubic centimeter per minute at standard temperature and pressure) is enough to protect the sidewalls for low Cl_2 fluxes but is insufficient for higher Cl_2 fluxes.

VII. IMPROVED PROCESS AND CONCLUSION

As we are aiming for applications in the low refractive index system, deep holes are crucial. Using the knowledge we gained, we optimized the process for deep holes presented in Fig. 8. The holes have depths of 4.2, 3.8, and 2.9 μm for diameters of 417, 310, and 180 nm, respectively. The parameters of Table I are used, with Cl_2 and N_2 fluxes of 15 and 2.9 SCCM, respectively.

To summarize, we have investigated the impact of the plasma power, pressure, and plasma chemistry on the etching of structures and holes for PhCs in InP/InGaAsP/InP. Samples were compared in terms of maximal achievable hole depth, hole shape, surface roughness, and undercut.

The chemistry of the plasma has been identified as the most crucial etching parameter. Deep holes can be achieved with a highly chemical process, demanding a high Cl_2 content. However, pure Cl_2/Ar plasmas at 200 °C are not capable of forming a passivation layer at the sidewalls, which results in a lateral etching of the semiconductor below the mask. Adding a small amount of nitrogen prevents the undercut but is detrimental for surface quality, as it promotes roughness at the sidewalls and at the bottom of large-area structures. Therefore a delicate balance needs to be found.

The rf and ICP powers should be kept low to achieve deep holes by reducing the etch rate and giving the reaction species time to sublimate and diffuse out of the holes. Our findings can be summarized in the following qualitative etch model displayed in Table IV.

ACKNOWLEDGMENTS

This work was carried out in the framework of the European Network of Excellence ePIXnet and the Swiss National Science Foundation program NCCR Quantum Photonics. Devices were fabricated at the FIRST Center of Micro- and Nanoscience of the ETH Zurich. The authors would like to acknowledge E. Gini (FIRST) for the epitaxy and O. Homan (FIRST) for technical support.

[1] J. D. Joannopoulos, R. D. Meade, and J. N. Winn, *Photonic Crystals—Molding the Flow of Light* (Princeton University Press, Princeton, 1995), pp. 1–137.
[2] F. Robin *et al.*, Proc. SPIE **6124**, 612415 (2006).
[3] T. F. Krauss, Phys. Status Solidi A **197**, 688 (2003).
[4] A. Talneau, L. L. Gouezigou, and N. Bouadma, Opt. Lett. **26**, 1259 (2001).
[5] M. Mulot, S. Anand, M. Swillo, M. Qiu, B. Jaskorzynska, A. Talneau, L. L. Gouezigou, and N. Bouadma, J. Vac. Sci. Technol. B **21**, 900 (2003).
[6] C. F. Carlström, R. v. d. Heijden, F. Karouta, R. W. v. d. Heijden, H. W. M. Salemink, and E. v. d. Drift, J. Vac. Sci. Technol. B **24**, L6 (2006).
[7] K. Rauscher, thesis ETH Zurich, 2006.
[8] M. Mulot, S. Anand, C. F. Carlström, M. Swillo, and A. Talneau, Phys. Scr., T **T101**, 106 (2002).
[9] R. Ferrini, A. Berrier, L. A. Dunbar, R. Houdré, M. Mulot, S. Anand, S. d. Rossi, and A. Talneau, Appl. Phys. Lett. **85**, 3998 (2004).
[10] R. Ferrini, B. Lombardet, B. Wild, R. Houdre, and G.-H. Duan, Appl. Phys. Lett. **82**, 1009 (2003).
[11] H. Benisty, D. Labilloy, C. Weisbuch, C. J. M. Smith, T. F. Krauss, D. Cassagne, A. Béraud, and C. Jouanin, Appl. Phys. Lett. **76**, 532 (2000).
[12] M. V. Kotlyar, T. Karle, M. D. Settle, L. O'Faolain, and T. F. Krauss, Appl. Phys. Lett. **84**, 3588 (2004).
[13] J. F. Holzman, P. Strasser, R. Wüest, F. Robin, D. Erni, and H. Jäckel, Proceedings of the 17th International Conference of IPRM, 2005, p. 570
[14] P. Strasser, R. Wüest, F. Robin, K. Rauscher, B. Wild, D. Erni, and H.

Jäckel, Proceedings of the 17th International Conference of IPRM, 2005, p. 242
[15]R. Ferrini, D. Leuenberger, M. Mulot, M. Qiu, J. Moosburger, M. Kamp, A. Forchel, S. Anand, and R. Houdré, IEEE J. Quantum Electron. **38**, 786 (2002).
[16]R. Wüest, P. Strasser, F. Robin, D. Erni, and H. Jäckel, J. Vac. Sci. Technol. B **23**, 3197 (2005).
[17]G. Z. Yin and D. W. Jille, Solid State Technol. **30**(5), 127 (1987).
[18]P. Strasser, R. Wüest, F. Robin, C. Widmeier, D. Erni, and H. Jäckel, Proceedings of the 16th International Conference of IPRM, 2004 p. 175.
[19]R. v. d. Heijden *et al.*, Proceedings of the Symposium of IEEE/LEOS, 2004, p. 287.
[20]J. Lin, A. Leven, N. G. Weimann, Y. Yang, R. F. Kopf, R. Reyes, Y. K. Chen, and F.-S. Choa, J. Vac. Sci. Technol. B **22**, 510 (2004).
[21]A. Matsutani, H. Ohtsuki, F. Koyama, and K. Iga, Jpn. J. Appl. Phys., Part 1 **38**, 4260 (1999).
[22]R. A. Gottscho, C. W. Jurgensen, and D. J. Vitkavage, J. Vac. Sci. Technol. B **10**, 2133 (1992).
[23]R. v. d. Heijden *et al.*, Proc. SPIE **5450**, 523 (2004).